

# A Planar Fluxgate Magnetic Sensor for On-Chip Integration

Sang On Choi, Shoji Kawahito<sup>1</sup>, Kinya Takahashi<sup>1</sup>,  
Yoshinori Matsumoto, Makoto Ishida and Yoshiaki Tadokoro<sup>1</sup>

Department of Electrical and Electronic Engineering, Toyohashi University of Technology,  
Tempaku-cho, Toyohashi 441, Japan

<sup>1</sup>Department of Information and Computer Sciences, Toyohashi University of Technology,  
Tempaku-cho, Toyohashi 441, Japan

(Received March 11, 1996; accepted January 13, 1997)

**Key words:** magnetic sensor, fluxgate, integration, magnetic field analysis

In this paper, we present a planar fluxgate magnetic sensor for on-chip integration using silicon process technology. The fabrication process is simplified by using a newly developed sensing element which is composed of thin-film ferromagnetic cores at the top layer, and excitation and differential pick-up coils. The sensor core used is permalloy film deposited by sputtering. The coils are fabricated using a two-layer metallization process. The fabrication process for the sensing element is suitable for integrating the on-chip interface circuits. In order to achieve the optimum excitation condition, the sensing element structure is investigated by means of computation analysis. The sensing element is fabricated with 2- $\mu\text{m}$ -thick, 1400- $\mu\text{m}$ -long cores and excitation and pick-up coils (25 turns each). The sensing element fabricated using planar technology has a magnetic sensitivity of about 73 V/T at an excitation frequency of 1 MHz and a driver current of 150 mA<sub>p-p</sub>.

## 1. Introduction

One of the attractive features of silicon sensors lies in the monolithic integration of the sensor interface circuits with the sensing elements on the same chip.<sup>(1,2)</sup> However, the performance of the sensor depends on the material used, and silicon is not always suitable as a high-resolution magnetic sensing material. A possible solution to this problem is the combination of ferromagnetic materials and silicon technology. The fluxgate has potential

as a highly-sensitive magnetic sensor.<sup>(3)</sup> Fluxgate sensors using magnetic thin film and silicon-based technology have recently been reported.<sup>(4-8)</sup> If a fluxgate sensor integrated with on-chip signal conditioning circuits is developed by silicon process technology, we can expect various interesting applications because of its attractive features such as small size, light weight, high sensitivity and high resolution.

In this paper, we present a planar fluxgate magnetic sensor for on-chip integration using silicon process technology. The sensing element is composed of thin-film ferromagnetic cores at the top layer, and excitation and differential pick-up coils. Spiral-shaped coils are employed in the fluxgate sensing element. The sensing element structure is investigated by means of computation analysis of the magnetic field in the thin-film core.

Aluminum is used as the coil wire material due to its compatibility with the integrated circuit process. The first aluminum layer is used for the differential pick-up coil wire. The second aluminum layer is used for the excitation coil wire. The permalloy thin film is deposited by sputtering at the top layer. This fabrication process technology is effective for integrating the fluxgate sensor with the sensor interface circuit on the same chip. The fabricated sensing element has higher sensitivity than the conventional silicon magnetic sensor. The structure, magnetic field analysis, fabrication and experimental results are discussed in the following sections.

## **2. Structure of Sensing Element**

The basic configuration of the fluxgate sensing element is shown in Fig. 1. The sensing element is composed of two thin-film ferromagnetic cores, an excitation coil and a differential pick-up coil. The sensor core is excited by an a.c. magnetic field with a triangular waveform which is generated by the excitation coil. The peak magnetic field should be large enough to saturate the core. When the external magnetic field is zero, the induced voltage of the pick-up coil is cancelled due to opposite excitation. When a d.c. external magnetic field is applied parallel to the core-axis direction, pulse voltage appears at the pick-up coil due to the phase shift of the induced pulse. The external magnetic field can be measured by detecting this phase shift. A typical sensing principle is based on the fact that even harmonics, especially the second harmonic, are produced in the pick-up coil when the induced pulse phase is shifted due to the external magnetic field.

Figure 2 shows the structure of the differential fluxgate sensing element fabricated using silicon process technology based on the configuration shown in Fig. 1. The coil structure is formed using a two-layer metallization process using aluminum. The first aluminum layer (under layer) is for the pick-up coil, and the second aluminum layer is for the excitation coil. A ferromagnetic film (permalloy) is deposited by sputtering at the top layer. These conductive layers are insulated by polyimide films.

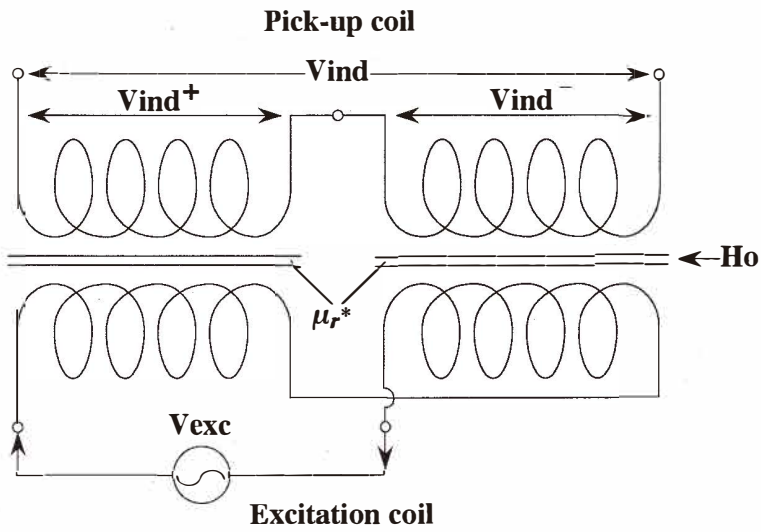


Fig. 1. Basic configuration of the fluxgate sensor.

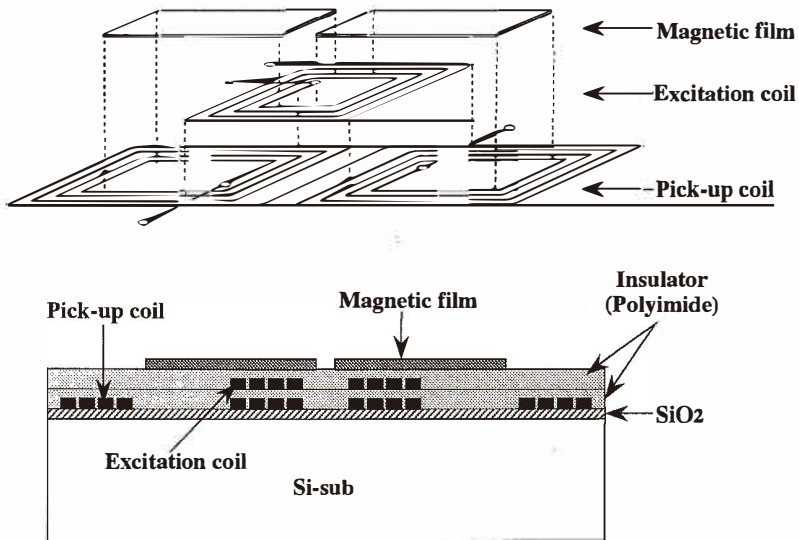


Fig. 2. Structure of the differential fluxgate sensing element.

### 3. Magnetic Field Analysis

Figure 3 shows the magnetic field distribution in the thin-film core excited by the single-turn coil.<sup>(9)</sup> The magnetic field in the core-axis direction is given by

$$\begin{aligned}
 H(x) &= \frac{I}{a} \left( 1 - e^{-\frac{a}{2\lambda}} \cosh \frac{x}{\lambda} \right) \quad \left( |x| < \frac{a}{2} \right), \\
 H(x) &= \frac{I}{a} \sinh \left( \frac{a}{2\lambda} \right) e^{-\frac{x}{\lambda}} \quad \left( |x| > \frac{a}{2} \right),
 \end{aligned} \tag{1}$$

where  $a = 20 \mu\text{m}$ ,  $\lambda^2 = gt\mu_r/2$ ,  $g = 6 \mu\text{m}$ ,  $t = 2 \mu\text{m}$ ,  $w = 700 \mu\text{m}$ , and the effective permeability  $\mu_r = 750$ . The excitation current  $I$  is 75 mA. In the case of thin-film core, the leakage flux is large and the magnetic field rapidly decreases as the distance from the excitation coil is increased. Therefore, the excitation coil wires should be periodically wound at short intervals and the pick-up coil wires should be wound in such a way that they overlap with the excitation wires for effective excitation.

The configuration of the  $N$ -turns coil is shown in Fig. 4. The magnetic field of the  $i$ th turn only in the core-axis direction is given by

$$\begin{aligned}
 H_i(x) &= \frac{I}{a} \sinh \frac{a}{2\lambda} e^{-\frac{x-(i-1)(a+b)}{\lambda}} \quad \left( (i-1)(a+b) - \frac{a}{2} > x \right), \\
 H_i(x) &= \frac{I}{a} \left( 1 - e^{-\frac{a}{2\lambda}} \cosh \frac{x-(i-1)(a+b)}{\lambda} \right) \\
 &\quad \left( (i-1)(a+b) - \frac{a}{2} \leq x \leq (i-1)(a+b) + \frac{a}{2} \right), \\
 H_i(x) &= \frac{I}{a} \sinh \frac{a}{2\lambda} e^{-\frac{x-(i-1)(a+b)}{\lambda}} \quad \left( (i-1)(a+b) + \frac{a}{2} < x \right).
 \end{aligned} \tag{2}$$

Therefore, the magnetic field generated by the  $N$ -turns coil in the core-axis direction is given by

$$H(x) = \sum_{i=1}^N H_i(x). \tag{3}$$

Figure 5 shows the magnetic field distributions in the core-axis direction according to the number of turns of the excitation coil and the current for optimum excitation. The core

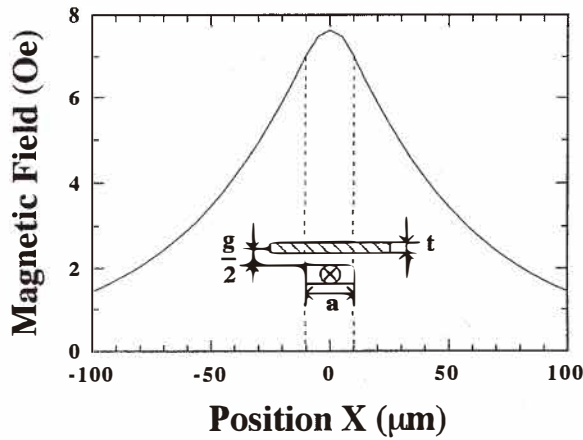


Fig. 3. Magnetic field distribution in the thin-film core excited by the single-turn coil.

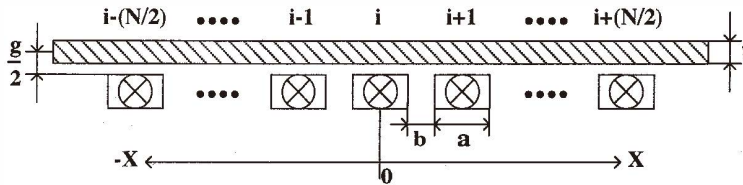


Fig. 4. Configuration of the  $N$ -turns coil.

thickness  $t$  and the coil gap  $g$  are assumed to be  $6 \mu\text{m}$  and  $2 \mu\text{m}$ , respectively. The core length is assumed to be infinitely long. The wire pitch is width ( $a$ )/space ( $b$ ) =  $20 \mu\text{m}/5 \mu\text{m}$ , and the effective permeability  $\mu_r$  is 750. An excitation current of 75 mA is used in Fig. 5(a). The magnetic fields saturate at 37.5 Oe as the number of turns of the excitation coil is increased. The number of excitation coil turns used in Fig. 5(b) is 25. The coil is wound within the range of  $-310 \mu\text{m}$  to  $310 \mu\text{m}$ . The magnetic fields increase as the excitation currents are increased.

In an ideal spiral coil structure, the magnetic field generated by the coil near the coil surface is given by

$$H = \frac{I}{P} \tag{4}$$

where  $I$  is the excitation current and  $P$  is the coil wire pitch. The optimum excitation

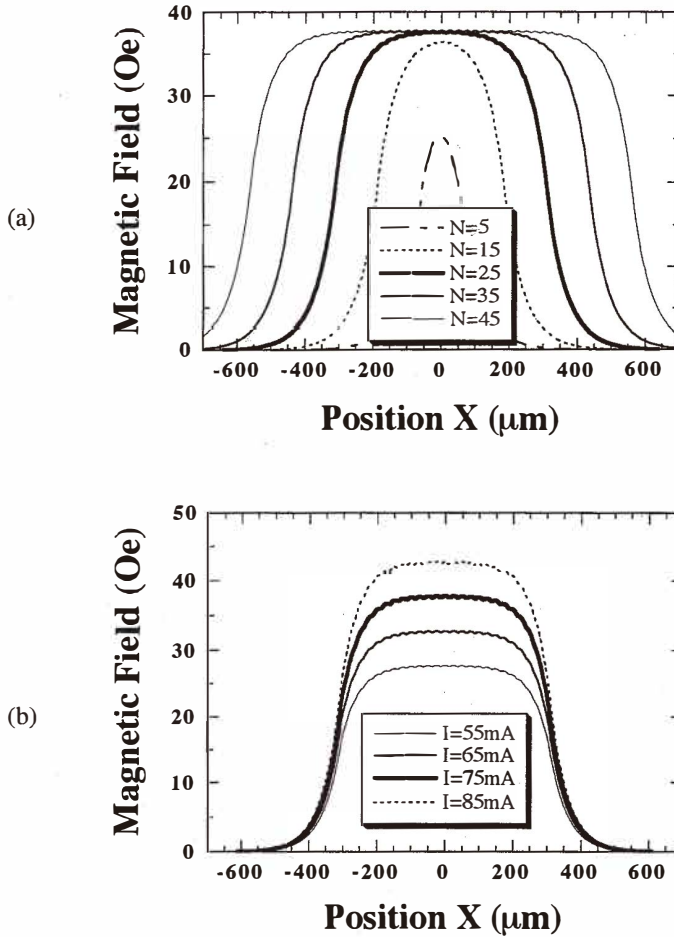


Fig. 5. Magnetic field distributions in the core-axis direction. (a) Number of turns of excitation coil (excitation current of 75 mA), and (b) excitation current (excitation coil of 25 turns).

condition to obtain the highest sensitivity in second harmonic detection is  $H_m = 2H_s$  where  $H_m$  is the peak excitation magnetic field and  $H_s$  is the saturation magnetic field. Therefore,  $H_m$  for the optimum excitation condition is calculated to be 37.5 Oe with  $I = 75$  mA and  $P = 25$   $\mu\text{m}$ . Wire resistance increases as the number of coil turns increases. From Fig. 5, the magnetic field distributions with the parameters of  $I = 75$  mA,  $N = 25$ ,  $a = 20$   $\mu\text{m}$ ,  $b = 5$   $\mu\text{m}$  agree with the ideal value. Therefore, we selected the design parameters shown in Table 1.

Table 1  
Design parameters of sensing element.

Excitation coil turns	25 turns
Excitation current	75 mA
Coil wire width	20 $\mu\text{m}$
Coil wire spacing	5 $\mu\text{m}$
Coil gap	6 $\mu\text{m}$
Core thickness	2 $\mu\text{m}$
Effective permeability	750

#### 4. Fabrication

The fabrication process is shown in Fig. 6. A 1.0- $\mu\text{m}$ -thick  $\text{SiO}_2$  film is grown by wet oxidation on the silicon wafer. The pick-up coil wire of the sensing element is fabricated using the first aluminum layer of about 2.2  $\mu\text{m}$  thickness. The aluminum layer is deposited by sputtering and patterned by photolithography and reactive ion etching (RIE) using  $\text{BCl}_3/\text{O}_2/\text{CHCl}_3$  gases. For insulation and planarization, a polyimide film is used. To obtain a planar surface, the polyimide is coated and baked three times. After that, the film is dry-etched to about 2  $\mu\text{m}$  with  $\text{O}_2/\text{CF}_4$  gases. Via holes are formed to contact the second-layer wires to the first-layer wires. The second aluminum layer of about 3.5  $\mu\text{m}$  thickness is used for the excitation coil. This aluminum layer is also deposited by sputtering and patterned by RIE. For insulation and planarization, a polyimide film is used and the film is then etched again. Permalloy film (81% Ni, 19% Fe) is deposited on the top layer using high-rate, low-temperature facing-targets sputtering.<sup>(10)</sup> After that, the permalloy film is patterned by photolithography and chemical etching using commercially available etchant for NiFe at a bath temperature of 32°C.

Figure 7 shows a micrograph of the planar fluxgate sensor fabricated by silicon process technology and deposition of ferromagnetic thin film. The area of the sensing element is  $4.2 \times 2.1 \text{ mm}^2$ .

#### 5. Characteristics

A fluxgate sensor shown in Fig. 2 was fabricated. The number of turns of the differential pick-up coil and the excitation coil is 25 each. The core has a thickness of 2  $\mu\text{m}$ , a length of 1400  $\mu\text{m}$ , and a width of 700  $\mu\text{m}$ . The wire pitch of the coil is 25  $\mu\text{m}$  with 20  $\mu\text{m}$  line and 5  $\mu\text{m}$  spacing. The resistances of the pick-up coil and excitation coil are 100  $\Omega$  and 255  $\Omega$ , respectively.

Figure 8 shows the B-H loops of the sputtered permalloy core measured using a VSM (vibrating sample magnetometer). Figures 8(a) and 8(b) correspond to the B-H loops of the patterned core on the silicon substrate covered by polyimide film and the core of the actually fabricated fluxgate sensing element, respectively. The dimensions of the core are

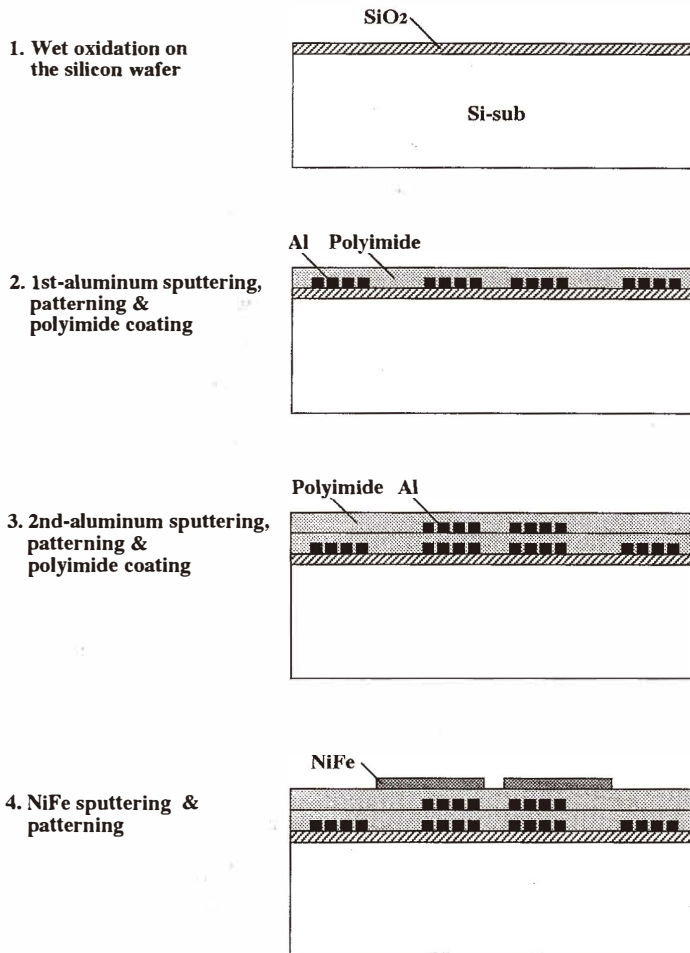


Fig. 6. Fabrication process.

length  $1400\ \mu\text{m}$ , width  $700\ \mu\text{m}$ , and thickness  $2\ \mu\text{m}$ . From these B-H loops, the d.c. permeability and coercive force, respectively, are about 1200 and 31 A/m for Fig. 8(a), and 750 and 32 A/m for Fig. 8(b). The degradation of the permeability of the core in the sensing element is due to the lack of flatness of the substrate. The coil wire pattern greatly affects the flatness. The use of dummy metal to obtain a planar surface under the core will enhance the effective permeability.

At a driver current of  $150\ \text{mA}_{\text{pp}}$  and an excitation frequency of 1 MHz, the relationship between the applied d.c. external magnetic flux density and the induced second harmonic

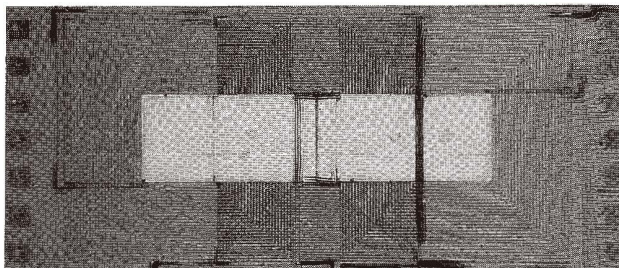


Fig. 7. Micrograph of the planar fluxgate sensor.

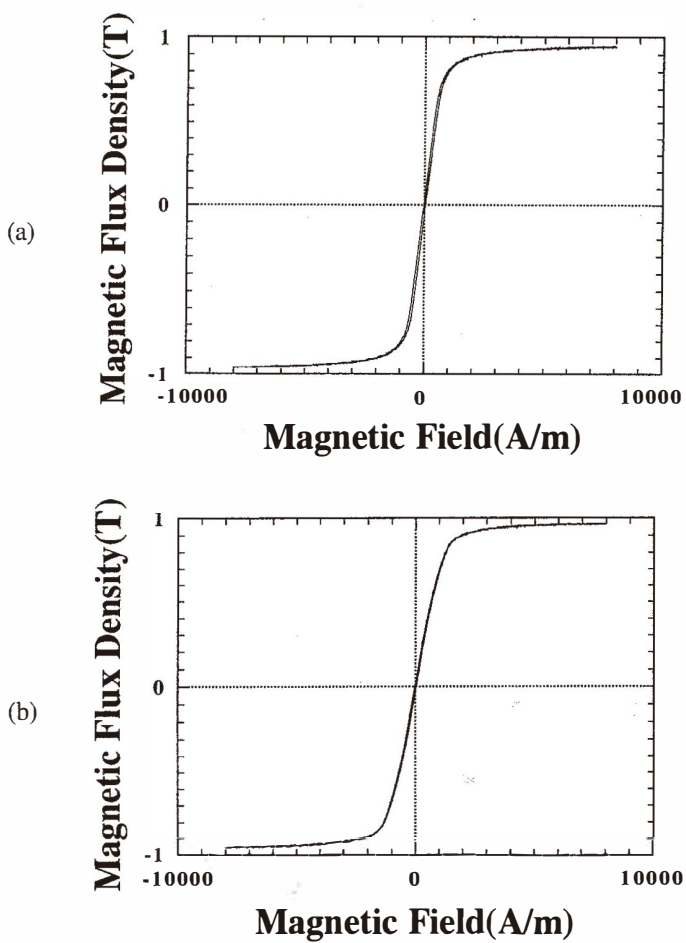


Fig. 8. B-H loops of permalloy core. (a) Core on silicon substrate, and (b) core of the fabricated fluxgate sensing element.

voltage is measured as shown in Fig. 9. The external magnetic field was applied parallel to the core-axis direction. In the measured range between  $-65 \mu\text{T}$  and  $65 \mu\text{T}$ , good linearity with no hysteresis is obtained.

For the characterization of the fluxgate sensing element, the core was first excited by a triangular current waveform through the excitation coil, and then the amplitude of the second harmonic of the pick-up coil output was measured using a FFT spectrum analyzer. The excitation frequency dependence of the sensitivity is shown in Fig. 10. The driver current is  $150 \text{ mA}_{\text{p-p}}$ . The sensitivity increases linearly as the excitation frequency increases to around 1 MHz. Figure 10 indicates that the highest sensitivity of the sensing element is about  $73 \text{ V/T}$  at 1 MHz. This value is considerably high when compared to that of the conventional silicon magnetic sensor.

The excitation current dependence of the sensitivity of the fluxgate sensor is shown in Fig. 11. The excitation frequency is 1 MHz. Figure 11 indicates that the optimum excitation current is about  $150 \text{ mA}_{\text{p-p}}$ . In an ideal spiral coil structure,  $H_m$  for the optimum condition is calculated to be  $3000 \text{ A/m}$  with  $I = 75 \text{ mA}$  and  $P = 25 \mu\text{m}$ . This value agrees with the condition  $H_m = 2H_s$ , since  $H_s$  of the sensor core is about  $1500 \text{ A/m}$  from the B-H loop of the core shown in Fig. 8(b).

## 6. Conclusions

In this paper, we present a planar fluxgate magnetic sensor suitable for integrating sensor interface circuits on the same chip. A sensing element with two-layer spiral coils and permalloy films at the top layer is developed, and is favorable for fabricating a fluxgate

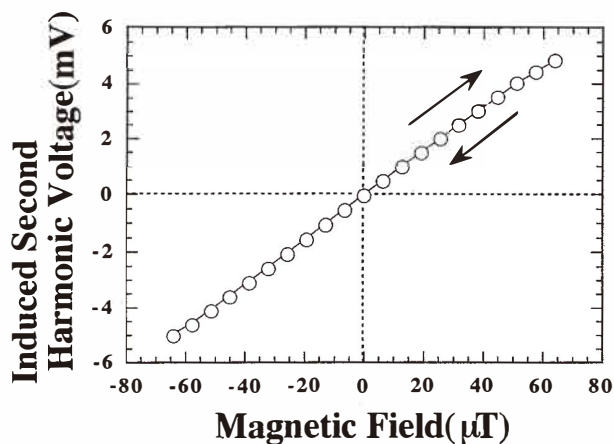


Fig. 9. Relationship between the applied d.c. external magnetic flux density and the induced second harmonic voltage.

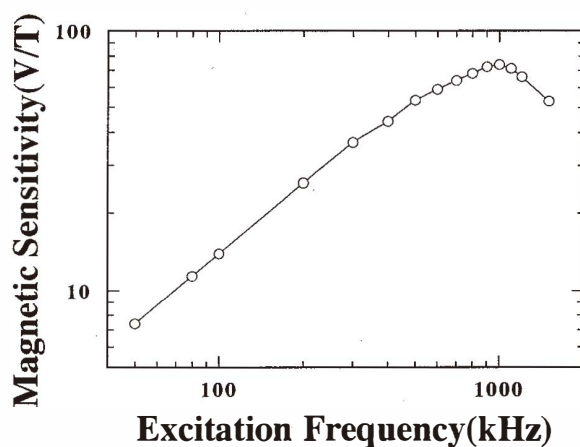


Fig. 10. Excitation frequency dependence of the sensitivity.

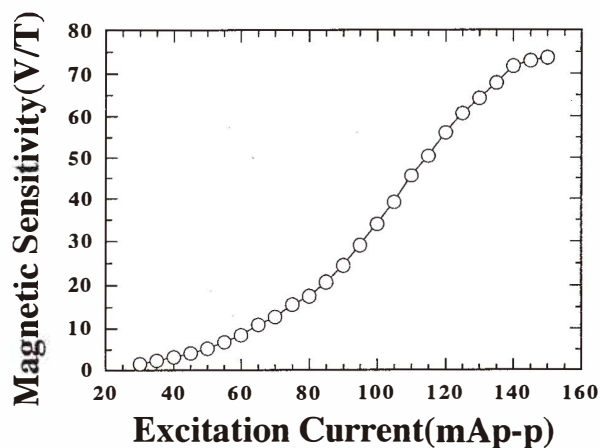


Fig. 11. Excitation current dependence of the sensitivity.

magnetic sensor integrated with on-chip interface circuits because of the simplicity of the fabrication process. In order to achieve the optimum excitation condition, the sensing element structure is investigated by means of computation analysis of the magnetic field in the thin-film core. The highly sensitive planar fluxgate sensor can be used for various interesting applications because the developed sensor covers a magnetic field detection range which cannot be matched by the conventional silicon magnetic sensor.

### Acknowledgments

The authors would like to thank Mr. M. Ashiki of Toyohashi University of Technology for his assistance in experiments. They also wish to thank Mr. A. Takayama and Mr. M. Tomita of Minebea Company for helpful discussion. This work was supported by a Grant-in-Aid for Young Scientists no. 09750490 from the Ministry of Education, Science and Culture of Japan.

### References

- 1 T. Nakamura and K. Maenaka: *Sensors and Actuators* **A21–A23** (1990) 762.
- 2 S. Kawahito, K. Hayakawa, Y. Matsumoto, M. Ishida and Y. Tadokoro: *Sensors and Materials* **8** (1996) 001.
- 3 P. Ripka: *Sensors and Actuators* **A33** (1992) 129.
- 4 T. Seits: *Sensors and Actuators* **A21–A23** (1990) 799.
- 5 S. Kawahito, Y. Sasaki, H. Sato, S. O. Choi, T. Nakamura and Y. Tadokoro: *Sensors and Materials* **5** (1994) 241.
- 6 S. Kawahito, H. Sato, M. Sutoh, and Y. Tadokoro: *Tech. Dig., Int. Conf. on Solid-State Sensors and Actuators* (1995) p. 290-A12.
- 7 K. Yoshimi, T. Munaka, H. Nakanishi, K. Iijima and Y. Yamada: *Tech. Dig., Sensor Symposium* (1995) p. 97.
- 8 R. Gottfried-Gottfried, W. Budde, R. Jähne, H. Küick, B. Sauer, S. Ulbricht, U. Wende: *Tech. Dig., Int. Conf. on Solid-State Sensors and Actuators* (1995) p. 289-A12.
- 9 R. E. Jones, Jr.: *IEEE Trans. Magn.*, **MAG14**, 5 (1978) 509.
- 10 Y. Hoshi, M. Kojima, M. Naoe, and S. Yamanaka: *IEICE J65-C* (1982) 783.